Available online at www.sciencedirect.com
ScienceDirect
Geochimica et Cosmochimica Acta 70 (2006) 6136–6152
Geochimica
www.elsevier.com/locate/gca

Kinetic model of olivine dissolution and extent of aqueous alteration on Mars

Julie D. Stopar [a,*], G. Jeffrey Taylor [a,b], Victoria E. Hamilton [a], Lauren Browning [c]

[a] *Hawaii Institute of Geophysics and Planetology, 1680 East-West Road, University of Hawaii, Honolulu, HI, USA*
[b] *NASA Astrobiology Institute, University of Hawaii, HI, USA*
[c] *Browning Research, 9014 Saddle Dr., San Antonio, TX 78255, USA*

Received 9 November 2005; accepted in revised form 31 July 2006

Abstract

If water was ever present on Mars, as suggested by geomorphological features, then much of the surface and subsurface may have experienced chemical weathering. Among those materials most readily altered is olivine, which has been identified on the Martian surface with IR spectroscopy and Mossbauer techniques and occurs in Martian meteorites. We use geochemical models of olivine dissolution kinetics to constrain the residence time of olivine on the surface of Mars in the presence of liquid water. From these models, we have calculated maximum dissolution rates and minimum residence times for olivine as a function of temperature, pH, Fe-composition, and particle size. In general, the most favorable conditions for olivine dissolution are fayalite-rich compositions, small particle sizes, high temperatures, and acidic solutions that are far from equilibrium. The least favorable conditions for olivine dissolution are forsterite-rich compositions, large particle sizes, ultra-low temperatures, and a neutral pH solution near equilibrium. By using kinetic models of olivine dissolution to bound dissolution rates and residence times, we can make inferences about the temporal extent of aqueous alteration on the surface of Mars. Under favorable conditions (pH 2, 5 °C, and far from equilibrium) a relatively large 0.1 cm (radius) particle of Fo_{65} composition can completely dissolve in 370 years. Particles may last 10^2–10^4 times longer under less favorable conditions. However, residence times of a few million years or less are small compared to the age of most of the Martian surface. The survival of olivine on the surface of Mars, especially in older terrains, implies that contact with aqueous solutions has been limited and wet periods on Mars have been short-lived.

1. Introduction

Aqueous alteration affects mineralogy through leaching, adsorption, dissolution, and formation of secondary phases. Therefore, it is important to understand the kinetics of aqueous alteration and mineral dissolution because they can provide information about the duration of aqueous processes and climate history. Morphological features on Mars such as gullies, valley networks, and outflow channels suggest at least the past presence of liquid water at the surface (e.g., Carr, 1996). Furthermore, an abundance of hydrogen in the subsurface detected by the Mars Odyssey Gamma Ray Spectrometer (GRS) suggests extant water ice in the upper half meter above ~60° latitude as well as hydrous minerals in equatorial regions (e.g., Boynton et al., 2002). If water was ever abundant for a significant time, then we might expect much of the surface to be chemically altered.

By studying the dissolution of primary minerals under simulated Martian conditions, we can begin to quantify the extent and duration of aqueous alteration. In particular, olivine is notorious for altering quickly in olivine-bearing basalts and is, therefore, a sensitive indicator of moderate amounts of aqueous alteration. Dissolution rates for olivine derived from laboratory experiments can be found in the literature (e.g., Wogelius and Walther, 1991, 1992; Pokrovsky and Schott, 2000a; Rosso and Rimstidt, 2000; Oelkers, 2001a). These experiments try to account

* Corresponding author. Fax: +1 808 956 6322.
E-mail address: jstopar@higp.hawaii.edu (J.D. Stopar).

0016-7037/$ - see front matter © 2006 Elsevier Inc. All rights reserved.
doi:10.1016/j.gca.2006.07.039

for various environmental factors such as pH, temperature, and atmospheric pressure. In this study, we use kinetic models derived from the laboratory experiments of Wogelius and Walther (1991, 1992) to constrain the residence time of olivine on Mars. By bounding dissolution rates and residence times, we can make inferences about the temporal extent of aqueous alteration. If olivine can be shown to alter quickly under Martian conditions, then the occurrence and preservation of olivine on the surface of Mars suggest limited interaction with water, at least locally.

2. Martian olivine

Olivine has been identified in varying abundances across the Martian surface (Christensen et al., 2000a; Hamilton and Christensen, 2003; Hoefen et al., 2003; Mustard et al., 2005; Koeppen and Hamilton, 2006) and is a minor component (~12% or less) of the basalt surface type identified by Christensen et al. (2000a). These basalts are observed over a widespread area but are concentrated mainly in the equatorial regions and Syrtis Major (Bandfield et al., 2000). In support of widespread, low-concentration olivine, the Mars Exploration Rover (MER) "Spirit" Mossbauer spectrometer and Mini-Thermal Emission Spectrometer (Mini-TES) at Gusev Crater identified olivine as a soil component (~15%, from Mini-TES) and as a component of the in situ rocks (Christensen et al., 2004a; Morris et al., 2004). The surface rocks are likely olivine basalts, some with light coatings and possible alteration rinds (e.g., Christensen et al., 2004a), and the Gusev soil is considered as being primarily derived from local olivine-basaltic rocks (e.g., Morris et al., 2004). The underlying mineralogy of rocks at Gusev Crater is modeled from Spirit's Alpha Particle X-Ray Spectrometer (APXS) to be 26–31 wt% olivine (McSween et al., 2004). Olivine was also identified by MER "Opportunity" in Meridiani Planum soil (Christensen et al., 2004b; Klingelhofer et al., 2004), illustrating that olivine can be a fairly common surface component (at low concentrations) probably due to the presence of olivine-bearing basalts and a basaltic component in the soil.

Although there is evidence to suggest the global distribution of olivine in relatively low concentrations on the surface of Mars, a few areas appear to contain higher olivine concentrations. Hoefen et al. (2003), Hamilton et al. (2003), and Koeppen and Hamilton (2006) used different methods to identify materials of higher olivine content (concentrations up to 30%) from Mars Global Surveyor Thermal Emission Spectrometer (TES) spectra. Hoefen and Clark (2001) estimate that ~3% of the Martian surface is covered with this olivine-rich material. The largest olivine-rich deposit (by area) is located near Nili Fossae northeast of Syrtis Major (Hamilton et al., 2003; Hoefen et al., 2003). Other "high" concentrations of olivine identified in TES data include (but are not limited to) the following locales: near the rims of Argyre and Hellas basins, on the southwest rim of Isidis Planitia, in southern Acidalia Planitia, near Terra Meridiani, in Aurorae Planum craters near Ganges Chasma, and in Ganges and Eos Chasmata (Hamilton et al., 2003; Hoefen et al., 2003). Olivine-rich materials were also identified with OMEGA in a wide variety of geologic units that include ancient terrains and younger terrains (Mustard et al., 2005).

Some Martian meteorites also contain substantial amounts of olivine. Olivine-bearing shergottites contain 7–29 vol % olivine, and lherzolitic shergottites contain 40–60 vol % olivine (Goodrich, 2002, and the references therein). The nakhlite meteorites generally contain 9–17 vol % olivine, except for MIL 03346 which contains ~3 vol % olivine (Treiman, 2005). The two chassignites, Chassigny and NWA 2737, are classified as dunites and contain ~90 vol % olivine (e.g., McSween and Treiman, 1998; Beck et al., 2006). While the Martian meteorites are not representative of the bulk of the observed Martian surface, the parent regions of these meteorites must also be olivine-bearing, and depending on the extent of their contact with liquid water, the olivine in these regions has experienced varying degrees of dissolution.

3. Dissolution processes and reactions

Olivine is a common anhydrous, rock-forming mineral with an isolated tetrahedral silicate structure (Deer et al., 1992). Fe^{2+} and Mg^{2+} cations are found in M1 and M2 sites within the olivine structure (e.g., Klein and Hurlbut, 1993). Six oxygen atoms surround each M-site cation, forming octahedra. The silica tetrahedra are isolated from each other by the surrounding M-site cations and are not linked together in chains, a characteristic of nesosilicate minerals. This allows the olivine structure to break down readily during dissolution. M1 sites, due to the increased deformation of their octahedral structure, are the most easily liberated during dissolution (Welch and Banfield, 2002). Olivine dissolves in water to release its components (Fe^{2+}, Mg^{2+}, and silica), which may precipitate in secondary minerals such as iddingsite (saponite and goethite), serpentine, smectite, goethite, maghemite, hematite, chlorides, sulfates, carbonates, or amorphous silica (Eggleton, 1986; Tosca et al., 2004).

In general, silicate dissolution is controlled by reactions at the mineral surface, but the mechanism of olivine dissolution remains a matter of current research (e.g., Pokrovsky and Schott, 2000a,b; Rosso and Rimstidt, 2000; Oelkers, 2001a; Welch and Banfield, 2002). Chemical alteration and dissolution usually occurs along crack boundaries and at defect sites in the crystal structure that can be accessed by aqueous solutions. Welch and Banfield (2002) found that dissolution of olivine always occurs in channels with orientation dependent on crystal axes, following the M-site cations.

The rate of dissolution can be limited in two general ways as described by Sak et al. (2004): (1) the availability of mineral surfaces at the water interface ("interface-limited") or (2) the availability of reactant (or product) to be

transported to/from the interface (“transport-limited”). If the alteration regime is transport-limited, dissolution is dependent on fluid flow (or diffusion), which might be restricted within channels or pore spaces.

Because olivine dissolution rates increase at low pH, it is likely that dissolution is controlled by the adsorption of protons onto the mineral surface, breaking cation–oxygen bonds and liberating silica tetrahedra (a process known as a protonation) (e.g., Oelkers, 2001b; Sak et al., 2004). Protonation between the mineral surface and the aqueous solution must occur before dissolution can proceed. The occurrence of this chemical interaction determines the locations of reactive surface sites and when dissolution can occur in the mineral structure. The number of reactive surface sites will limit dissolution.

4. Methodology

Due to the difficulty in observing dissolution mechanisms in action, mineral dissolution rates are determined from laboratory experiments and field data, or are inferred from microscopic observations. Rate equations are then fit to the data, taking into account as many environmental variables as possible (e.g., pH, temperature, atmospheric pressure, etc.). Here, we use dissolution rate equations derived from the laboratory experiments of Wogelius and Walther (1991, 1992) and extrapolate to Martian conditions. From the dissolution rates, we determine the minimum time needed to dissolve one olivine particle in each dissolution reaction as a function of particle size. This is similar to the mean lifetime calculations of Lasaga (1984) and Lasaga et al. (1994), except we consider the calculated residence times to represent minima instead of means, due to the numerous factors that can work to slow dissolution in natural environments (discussed in Sections 6.1–6.3). These calculated minimum residence times can then be compared to the estimated duration of aqueous processes on the surface of Mars to determine the likelihood of olivine survival in each situation.

4.1. Dissolution rates: the effects of pH, P_{CO_2}, temperature, and composition

The rate equations (Eqs. (1), (3)–(5) below) of Wogelius and Walther (1991, 1992) include the effects of temperature, pH, P_{CO_2}, and olivine composition. Wogelius and Walther used H_2O–HCl solutions in their experiments, and the influence of changing solution chemistry is ignored. The following equations were derived for low P_{CO_2} atmospheres ($\sim 3 \times 10^{-5}$ bar). For forsterite (Mg_2SiO_4) dissolution at pH 2–12, the rate constant (mol cm^{-2} s^{-1}) at standard temperature (25 °C) is:

$$R_{Fo} = 9.07(10^{-12}a_{H^+}^{0.54}) + 5.25(10^{-15}) + 2.33(10^{-17}a_{H^+}^{-0.31}) \quad (1)$$

$$a_{H^+} = 10^{(-pH)} \quad (2)$$

For fayalite (Fe_2SiO_4) dissolution at pH 2–7, the rate constant at standard temperature is:

$$R_{Fa} = 1.1(10^{-10}a_{H^+}^{0.69}) + 3.22(10^{-14}) \quad (3)$$

For fayalite dissolution at higher pH (8–12), the rate constant at standard temperature is:

$$R_{Fa} = 1.1(10^{-10}a_{H^+}^{0.69}) + 3.22(10^{-14}) + 1.2(10^{-16}a_{H^+}^{-0.3}) \quad (4)$$

For intermediate compositions along the fayalite–forsterite solid solution, the rate constant of dissolution at standard temperature can be obtained by summing the products of the mole fraction and the rate of dissolution of each endmember:

$$R_{Ol} = X_{Fa}R_{Fa} + X_{Fo}R_{Fo} \quad (5)$$

where X_{Fa} is the mole fraction fayalite, R_{Fa} is the fayalite rate constant (mol cm^{-2} s^{-1}), X_{Fo} is the mole fraction forsterite, and R_{Fo} is the forsterite rate constant (mol cm^{-2} s^{-1}).

For non-standard temperatures, we can calculate the rate constant of dissolution by rearranging the Arrhenius relationship:

$$\log R_2 = \log R_1 + E_a(T_1^{-1} - T_2^{-1})(2.303R)^{-1} \quad (6)$$

where is the R gas constant (1.987216 cal/K/mol), T_1 is the standard temperature (273.15 K), T_2 is the non-standard temperature (K), E_a is the activation energy (cal/mol), and R_1 is the rate constant of olivine dissolution at standard temperature (from Eqs. (1)–(5)), mol cm^{-2} s^{-1}, and R_2 is the rate constant of olivine dissolution at non-standard temperature (mol cm^{-2} s^{-1}).

Wogelius and Walther (1992) calculated an activation energy (E_a) of ~19,000 cal/mol. In order to calculate dissolution rates for Martian olivine from Eqs. (1)–(6), we need to determine reasonable values for pH, temperature, and olivine composition on Mars.

Determining a valid pH range for Mars is important because pH has a strong effect on olivine dissolution rates. Olivine of any composition dissolves more readily under very acidic conditions and more slowly at near-neutral pH (Wogelius and Walther, 1992). In low P_{CO_2} atmosphere, olivine of any composition also dissolves more readily at basic pH than near pH 7 (Wogelius and Walther, 1991). Aqueous solutions are generally considered to be acidic on Mars (e.g., Burns, 1993), and jarosite, an iron-sulfate stable between approximately pH 2–4 (Langmuir, 1997), is predicted as a potential alteration product on the surface of Mars (e.g., Burns, 1993; Newsom et al., 1999). Jarosite detected by the Mossbauer spectrometer onboard the 2004 Mars Exploration Rover “Opportunity” (Klingelhofer et al., 2004) is good evidence for the presence of some very low pH aqueous solutions. Here we consider a wider range of pH; however, we generally assume that a pH of 2–4 is most representative of Martian aqueous solutions.

Thus far, we have only discussed dissolution rates and residence times calculated from deoxygenated (low P_{CO_2}) experiments. However, Wogelius and Walther (1991) ob-

served dissolved CO_2 reacting with surface Mg in forsteritic olivine studies. They witnessed a slowing of the overall dissolution rate during this process for pH > 7. Eqs. (1)–(3), presented above, apply only to low $P_{CO_2} \leqslant 3.2 \times 10^{-5}$ bar (vs. terrestrial $P_{CO_2} \sim 3.5 \times 10^{-4}$ bar). At terrestrial P_{CO_2} and pH >7, forsterite dissolution rates appear to be independent of pH and remain approximately equal to the dissolution rate at pH 7 (Wogelius and Walther, 1991). Experimental data are not available for olivine dissolution at Martian P_{CO_2}, and we do not attempt to adjust the rate equations for the even higher P_{CO_2} on Mars ($\sim 5 \times 10^{-3}$ bar). However, we might assume that the dissolution trends are better represented by the terrestrial P_{CO_2} experiments of Wogelius and Walther (1991) than their deoxygenated, low P_{CO_2} experiments (1991, 1992). Nonetheless, since Martian aqueous environments are expected to be acidic, the effects of P_{CO_2} in basic solutions are of less importance to our calculations.

Surface temperatures during the Viking missions were observed between 17 °C and −143 °C (Kieffer et al., 1977), and a standard temperature of 25 °C is not unreasonable as a maximum surface temperature near the equator. Therefore, low-temperature aqueous processes can be estimated as occurring between 0 and 25 °C. Brine solutions can remain liquid at even lower temperatures due to the addition of salts (or other dissolved species), which lower the freezing point of solution. The stability of liquid brine at low temperatures depends on its composition. Antarctic brines can form springs at temperatures below 0 °C (Andersen et al., 2002), and Antarctic $CaCl_2$ brines proposed by Burt and Knauth (2003) as an analog for Mars can remain liquid below −50 °C. Brines can also affect species activity coefficients, thereby influencing dissolution behavior. On the other hand, the addition of impact- or magmatically generated heat to subsurface water or ice could raise the temperature of the liquid until it vaporizes. Here, we consider a wide range of possible temperatures to model a variety of temperature regimes and geologic processes.

There are three sources of data on Martian olivine composition currently available: (1) compositions derived from orbital spectral features, (2) compositions of olivine in Martian meteorites, and (3) compositions derived from MER instruments. Hoefen et al. (2003) compared the thermal IR spectral features of terrestrial olivine to the olivine component in TES spectra in order to infer an olivine composition of $\sim Fo_{60}$–Fo_{70} for most of the olivine near the Nili Fossae region, while some olivine (concentrated in the northeast portion of the deposit) appears to have higher iron compositions ($<Fo_{60}$). The southwest portion of this region is more magnesian. More recently, Koeppen and Hamilton (2006) matched spectral features of several terrestrial olivine compositions (including Fo_{91}, Fo_{60-68}, and Fo_{58}) to TES features across the surface of Mars. Preliminary results indicate that more magnesian olivine (Fo_{91}) is found in the oldest terrains while younger olivine-bearing materials are more iron-rich. The Martian meteorite Chassigny has olivine with a composition $\sim Fo_{68}$ (Banin et al., 1992); NWA 2737 has olivine $\sim Fo_{79}$, and shergottite meteorites known to date have a wide range of olivine compositions (Fo_{25}–Fo_{81}), with most being $\sim Fo_{60}$–Fo_{75} (Goodrich, 2002 , and references therein). Olivine-bearing basaltic rocks in Gusev Crater are measured as $\sim Fo_{50-60}$ by the Mossbauer spectrometer (Morris et al., 2004). At Meridiani Planum the olivine soil component is estimated as Fo_{60} (Klingelhofer et al., 2004). The olivine is $\sim Fo_{45}$ in the subsurface soil and dark rocks as determined from TES spectra (Christensen et al., 2004b). Here, we use Fo_{65} to represent an average Martian olivine composition. Eq. (5) is used to calculate the dissolution rate for this composition.

4.2. Residence times, particle size, and surface area

From the rates of dissolution, we calculate the minimum time needed to dissolve one spherical particle of olivine (of varying particle sizes) not in contact with any others. We make a few additional simplifying assumptions: (1) the composition of the aqueous solution does not change with time, (2) surface coatings do not form (no precipitation of secondary minerals on olivine surfaces), (3) pH and temperature do not change with time, (4) the solution is dilute and far from equilibrium, and (5) water can react with all geometric surface area. In general, these assumptions tend to enhance dissolution (with the exception that decreasing temperatures or increasing pH over time would slow dissolution). "Real" dissolution conditions are likely to differ from these assumptions, and this is in part why we consider our residence times to be minima. The effects of these and other factors that influence dissolution rates and times will be discussed in later sections.

Dissolution rate constants are converted to residence times (seconds) by:

$$t = M_{Ol}(R_{Ol} * SA * wt_{mol})^{-1} \quad (7)$$

where M_{Ol} is the mass of one particle of olivine (or mass of olivine dissolved) calculated from the density and the volume of the particle, grams (g), R_{Ol} is the rate constant of olivine dissolution (mol cm^{-2} s^{-1}), SA is the geometric surface area of the particle (cm^2), and wt_{mol} is the molecular weight of olivine (g/mol).

To account for the change in particle size as dissolution progresses, we integrate over time. After integration, Eq. (7) simplifies to:

$$t = \rho * r * (R_{Ol} * wt_{mol})_{-1} \quad (8)$$

where ρ is the density of olivine particle (g/cm^3) and r is the radius of the olivine particle (cm).

Thus, the residence time of a spherical olivine particle is dependent on composition, radius, and the calculated rate of dissolution (from Eqs. (1)–(6)).

Determination of an average particle size for olivine on Mars is necessary in order to use Eq. (8). Hamilton and Christensen (2004, 2005) reported that a few of the strongest olivine thermal IR features in the Nili Fossae lie in

areas not dominated by bedrock and that these deposits have a thermal inertia of ~310 J/m^2/K/s$^{1/2}$. Using the methods of Presley and Christensen (1997) to estimate particle size from thermal inertia and thermal conductivity, the particle size of olivine-rich materials is estimated as ~1 to 2 mm in diameter (Hamilton and Christensen, 2005). While these particles may not consist of pure olivine, they do provide a reasonable upper limit on Martian olivine particle sizes.

The MI (Microscopic Imager) onboard the Spirit Rover provided grain sizes of soils from Gusev Crater. The fine soil sediments, which are typically basaltic in composition and thus partially composed of olivine or olivine-bearing particles, consist of both coarse, rounded particles 1–2 mm in diameter and finer particles <0.5 mm in diameter (Grant et al., 2004). However, even finer particles are present below the resolution of the MI (<100 μm) (Herkenhoff et al., 2004a). Some "megacrysts" are seen in MI frames of a rock nicknamed "Mazatzal" after exposure of the rock interior by the Rock Abrasion Tool (RAT) (McSween et al., 2004). These megacrysts are hypothesized to be olivine, and from McSween et al.'s Figure 3, particle sizes can be roughly approximated as ~0.75 mm, which is consistent with olivine grain sizes in shergottite meteorites. Goodrich (2002) estimates that olivine grains in two olivine-bearing shergottites are typically ~1 mm (for EETA 79001) and ~0.25 mm (for SaU 005) in length. At Meridiani Planum, both sand-size particles and lithic fragments (1–3 mm in size) are basaltic components of the soil (Soderblom et al., 2004). Here, we consider a wide range of olivine particle sizes from 2 cm to 2 μm in diameter; however, we generally provide calculations for 2 mm and 0.2 mm diameter particle sizes in the figures and tables presented below.

There are two generally accepted ways of calculating surface area from particle diameter: geometrically and by the Brunauer, Emmett, and Teller (BET) method. The BET method uses gas absorption to measure a complex surface area including etch pits and defects, etc. (e.g., Brantley, 2003). BET surface areas better account for natural features in olivine particles than geometric surface areas do. However, much of the BET surface area may not actually be involved in the reaction (especially near saturation where transport is limited), and the geometric surface area may better represent the reactive surface (White and Brantley, 2003). White and Brantley hypothesize that short-term experiments may be dominated by crystal defects, both naturally and mechanically created, and that these would be best quantified by BET surface areas. In longer duration reactions, deeper layers are exposed, which theoretically should contain fewer defects, and surface areas would be better represented geometrically. However, during the course of White and Brantley's six-year dissolution experiments, BET surface areas were observed to increase with time, translating to a decrease in dissolution rate over time (because dissolution rates are normalized to surface area). This potential change in rate with time, as well as ways to reconcile field (long-term) and laboratory (short-term) dissolution rates, is further discussed in Section 6 below. Unfortunately, study of the differences between reactive, geometric, and BET surface areas is difficult, and the duration of dissolution may affect the surface features of mineral particles. In Eq. (7) (above), surface area is assumed to be geometric and particles are defined as spheres because we do not currently have measurements of the BET surface area or the surface roughness of Martian olivine to estimate the BET surface area or how it changes over time.

5. Results: effects of pH, composition, temperature, and particle size

Our results suggest that even large particles (2 mm diameter) of olivine can weather quickly, especially at high temperatures and low pH. Calculated rates and residence times for various hypothetical Martian conditions are shown in Table 1.

Residence times are strongly affected by pH, which is an important control on dissolution rates. Fig. 1 shows the variation in minimum residence time with changing pH at a constant temperature. The difference between the calculated minimum residence times for relatively large olivine particles (radius = 0.1 cm) at pH of 2 and 7 is approximately a factor of 100 (with some variation depending on composition, temperature, and particle size discussed below). Lower pH solutions cause more rapid dissolution and, thus, result in shorter residence times. Relatively longer times are needed to dissolve an olivine particle at neutral pH than at either acidic or basic pH (except for olivine at terrestrial P_{CO2} and basic pH, as discussed below).

Solution pH on Mars is not well constrained, but a sensitivity analysis (Table 2) indicates that a small uncertainty in pH (±1 pH unit) will not produce a large uncertainty in calculated residence times. The largest uncertainties in calculated residence times result from large under- or over-estimates of solution pH (±2 or more pH units). As an example, olivine of Fo_{65} composition at 25 °C with a 0.1 cm radius and an uncertainty in pH of ±2 pH units results in residence times that differ by a factor of $<10^2$ (at pH 2 the calculated residence time is ~40 years, whereas at pH 6 the calculated residence time is ~3500 years). This uncertainty is large compared to the effects of reasonable uncertainties in olivine composition and reaction temperature, but small compared to other uncertainties (below).

The effect of composition is also shown in Fig. 1. From the difference in the three curves for fayalite (Fo_0), forsterite (Fo_{100}), and Fo_{65} olivine, it is apparent that relatively longer times are needed to dissolve an olivine particle with a given composition at neutral pH than at either low or high pHs (except at high P_{CO_2}, discussed below). Fe-rich olivine particles require less time to completely dissolve than Mg-rich particles of the same size at the same temperature and pH. Fayalite particles can dissolve approximately 10 times faster than forsterite particles under the same conditions.

Table 1
Selected maximum dissolution rates and minimum dissolution times for hypothetical Martian conditions (from the deoxygenated rate equations of Wogelius and Walther, 1992)

Composition	pH	Radius (cm)	T (°C)	Max. rate (mol cm^{-2} s^{-1})	Min. time (yrs)
Fa_{100}	2	0.1	−50	9.65×10^{-17}	5.2×10^{5}
			5	4.61×10^{-13}	110
			100	2.91×10^{-9}	0.02
	5	0.1	−50	1.49×10^{-18}	3.4×10^{7}
			5	7.10×10^{-15}	7100
			100	4.48×10^{-11}	1.1
Fo_{100}	2	0.1	−50	1.59×10^{-17}	6.2×10^{6}
			5	7.58×10^{-14}	1300
			100	4.78×10^{-10}	0.21
	5	0.1	−50	5.05×10^{-19}	2.0×10^{8}
			5	2.41×10^{-15}	4.1×10^{4}
			100	1.52×10^{-11}	6.5
Fo_{65}	2	0.1	−50	4.41×10^{-17}	1.8×10^{6}
			5	2.10×10^{-13}	370
			100	1.33×10^{-9}	0.06
		0.01	−50	4.41×10^{-17}	1.8×10^{5}
			5	2.10×10^{-13}	37
			100	1.33×10^{-9}	6.0 x10^{-3}
	3	0.1	−50	1.01×10^{-17}	7.7×10^{6}
			−25	7.57×10^{-16}	1.0×10^{5}
			5	4.83×10^{-14}	1600
			25	4.84×10^{-13}	160
			100	3.04×10^{-10}	0.26
		0.01	−50	1.01×10^{-17}	7.7×10^{5}
			5	4.83×10^{-14}	160
			100	3.04×10^{-10}	0.03
	5	0.1	−50	8.49×10^{-19}	9.1×10^{7}
			−25	6.36×10^{-17}	1.2×10^{6}
			5	4.05×10^{-15}	1.9×10^{4}
			25	4.06×10^{-14}	1900
			100	2.56×10^{-11}	3.0
		0.01	−50	8.49×10^{-19}	9.1×10^{6}
			5	4.05×10^{-15}	1900
			100	2.56×10^{-11}	0.30
	7	0.1	−50	3.86×10^{-19}	2.0×10^{8}
			5	1.84×10^{-15}	4.2×10^{4}
			100	1.16×10^{-11}	6.7
		0.01	−50	3.86×10^{-19}	2.0×10^{7}
			5	1.84×10^{-15}	4200
			100	1.16×10^{-11}	0.67

As composition has a smaller effect on residence times than pH, it follows that the calculations are less sensitive to uncertainties in olivine composition. Table 3 presents our sensitivity analysis for compositions between Fo_{20} and Fo_{80}. There is less than a factor of two difference in residence times between particles of Fo_{20} and Fo_{80} with 0.1 cm radii at pH 4 and 25 °C.

An increase in temperature decreases the amount of time necessary to completely dissolve an olivine particle (Fig. 2). For example, the residence time of a Fo_{65} particle at 5 °C is ~6000 times longer than for the same particle at 100 °C. At high temperatures, such as those found in hydrothermal systems, an olivine particle can dissolve in a few years. Relatively large particles (of intermediate composition, Fo_{65}) with a 0.1 cm radius can dissolve in fewer than 50,000 years at low temperatures (5 °C) and neutral pH, where rates are slowest. From Fig. 2, temperature is expected to have a

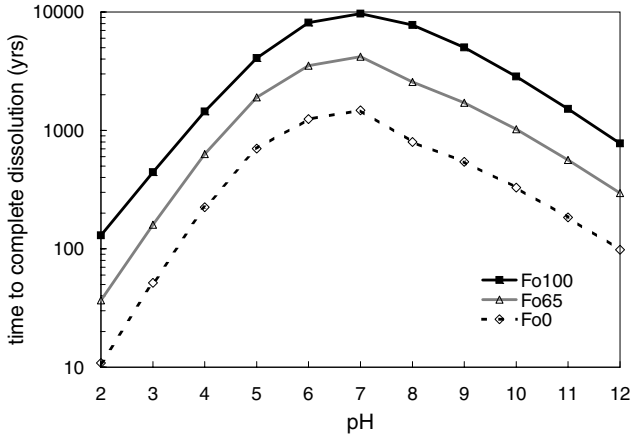

Fig. 1. Minimum time for complete dissolution of a single olivine particle at 25 °C. Residence time depends on pH, composition, P_{CO_2} (low $CO_2 \leqslant 3.2\times10^{-5}$ bars shown here), and particle size (only 0.1 cm radius particles are shown here).

large effect on dissolution rates and residence times. However, the sensitivity analysis for the effects of temperature variation given in Table 4 illustrates the relatively minor effect of temperature uncertainties on the overall predicted residence times. For a Fo_{65} olivine particle (radius 0.1 cm) at pH 4, there is a factor of ~10 difference in calculated minimum residence times between the same particle at 15 °C and 35 °C.

In general, olivine of Martian composition as modeled here is predicted to dissolve fairly rapidly at all temperatures above the freezing point of pure H_2O and should not last over geologic times if exposed to the liquid phase. The exception to this rapid dissolution may occur in ultra-low temperature brines. At such low temperatures, dissolution rates are very slow, and olivine particles can persist for several million years at neutral to slightly acidic pH.

Residence times for olivine particles at ultra-low temperatures (−50° and −25 °C) were extrapolated using the experimentally determined activation energy of Wogelius and Walther (1992). It is not clear that such an extrapolation is valid, but to our knowledge, no activation energy data are available for brine solutions at ultra-low temperatures. Experimentally determined activation energies for olivine vary in the literature (e.g., Grandstaff, 1986; Wogelius and Walther, 1992; Rosso and Rimstidt, 2000). Here we have used Wogelius and Walther's value of 19,000 cal/mol. Grandstaff published a value of ~9100 cal/mol, and Rosso and Rimstidt calculated a value of ~10,180 cal/mol. The reason for the variation between experiments is uncertain. Casey et al. (1993) suggested that solution pH during dissolution might affect activation energy. The activation energy used in our calculations affects dissolution rates at non-standard temperatures. Fig. 3 shows the variability in calculated dissolution rates and residence times for Martian olivine (Fo_{65}) as activation energy is altered. At the highest and lowest temperatures, residence times (and dissolution rates) have the largest dependence on the value of activation energy, thus extrapolation

Table 2
Sensitivity analysis[f] of pH for an olivine particle of Fo_{65} at 25 °C with radius = 0.1 cm

Estimated pH[a]	"Actual" pH[b]	Calculated residence time[c] (yrs)	Δ Residence time[d] (yrs)	Coefficient[e] (γ)
4 (Calculated residence time 632 yrs)	2	37	−595	17.08
	3	160	−472	3.95
	5	1906	1274	0.33
	6	3528	2896	0.18
	7	4195	4563	0.15

[a] The assumed or estimated pH. An estimated pH of 4 has a calculated residence time of 632 years under the given conditions.
[b] The hypothetical "actual" pH (e.g., the pH at a specific locale).
[c] The residence times (years) calculated at each "actual" pH. When the "actual" pH differs from the estimated pH, the calculated residence time will be accordingly longer or shorter than the residence time at the estimated pH (632 years at pH 4 under the given conditions).
[d] Δ residence time (years) is the difference between the calculated residence time at pH 4 (632 years) and the calculated residence time at the "actual" pH.
[e] The coefficient (γ) is the calculated residence time at pH 4 divided by the calculated residence time at the "actual" pH. For example, the difference (γ) in calculated residence times for the same particle at pH 4 and pH 2 under the given conditions is a factor of ~17.
[f] This table compares the calculated residence time for an assumed or estimated pH with the residence times calculated for a range of hypothetical "actual" pH values in order to show how uncertainty in pH affects the calculated residence times.

Table 3
Sensitivity analysis[f] of composition for an olivine particle at 25 °C and pH 4 with radius = 0.1 cm

Estimated Fo#[a]	"Actual" Fo#[b]	Calculated residence time[c] (yrs)	Δ Residence time[d] (yrs)	Coefficient[e] (γ_1)
65 (Calculated residence time 632 yrs)	80	864	232	0.73
	75	775	143	0.82
	70	698	66	0.91
	60	574	−58	1.10
	55	524	−108	1.21
	50	480	−152	1.32
	40	464	−168	1.36
	30	453	−179	1.39
	20	447	−185	1.42

[a] The assumed or estimated Fo#. An estimated olivine composition of Fo_{65} has a calculated residence time of 632 years under the given conditions.
[b] The hypothetical "actual" Fo# (e.g., the olivine composition at a specific locale).
[c] The residence times (years) calculated at each "actual" Fo#. When the "actual" Fo# differs from the estimated olivine composition, the calculated residence time will be accordingly longer or shorter than the residence time at the estimated Fo# (632 years for Fo_{65} under the given conditions).
[d] Δ residence time (years) is the difference between the calculated residence time for Fo_{65} (632 years) and the calculated residence time for the "actual" Fo#.
[e] The coefficient (γ) is the calculated residence time at Fo_{65} divided by the calculated residence time at the "actual" Fo#. For example, the difference (γ) in calculated residence times for a Fo_{80} particle and a Fo_{65} particle under the given conditions is a factor of ~1.4.
[f] This table compares the calculated residence times for an assumed or estimated Fo# with the residence times calculated for a range of hypothetical "actual" Fo#s in order to show how uncertainty in olivine composition affects the calculated residence times.

to sub-zero temperatures from activation energies based on standard temperature carries the largest amount of uncertainty and potential error. At −50 °C, more than 2 orders of magnitude change in residence time can be due to the uncertainty in value of activation energy alone.

Particle size is the factor that ultimately determines how long an olivine grain can survive in an aqueous environment. As expected, smaller particles dissolve in less time than larger particles because they have a higher surface to volume ratio, or "effective" surface area. Fig. 4 shows that for every factor of 10 increase in particle radius, the residence time also increases by a factor of 10 (as expected from Eq. (8)). However, one factor not quantitatively explored here is the effect of "reactive" surface area. It is possible that in many cases the surface area involved in dissolution is less than geometric (and BET) surface area. Velbel (1993) estimated that as little as 10% or less of the available surface area may actually be involved in dissolution reactions at any given time due to low porosity, low permeability, or a low water/rock ratio. For example, if dissolution only occurs at specific sites on the mineral surface, in channels or pore spaces, or if precipitates block reactive sites (potentially decreasing porosity), then not all geometric surface area may be available for reaction. This is one reason why the residence times we calculate are only minima. Even so, calculated olivine residence times only increase by a factor of 10 when reactive surface area is reduced to 10% of its original value (Fig. 5). Further discussion of natural vs. ideal conditions is provided in Section 6.3 below.

5.1. Total uncertainty

While there are numerous uncertainties about the process of olivine dissolution on Mars, conditions are not completely unconstrained. As discussed above, we can approximate olivine composition fairly well based on remote sensing data and meteorite studies. Furthermore,

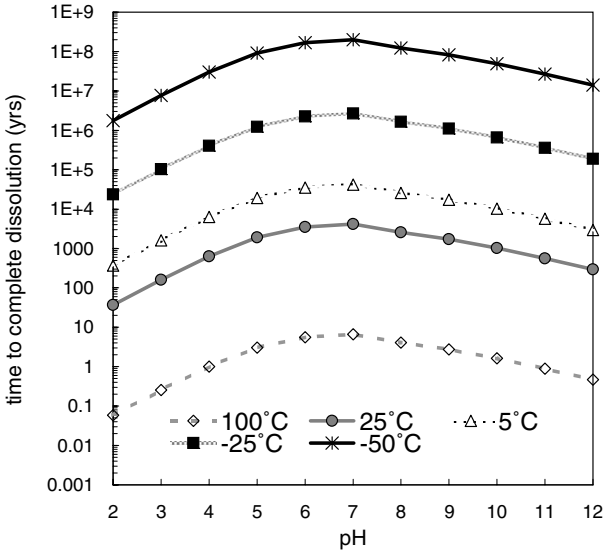

Fig. 2. Minimum time for complete dissolution of a single Fo_{65} particle at −50 °C, −25 °C, 5 °C, 25 °C, and 100 °C. Residence time depends on pH, P_{CO_2} (low $P_{CO_2} \leqslant 3.2 \times 10^{-5}$ bars shown here), and particle size (only 0.1 cm radius particles are shown here).

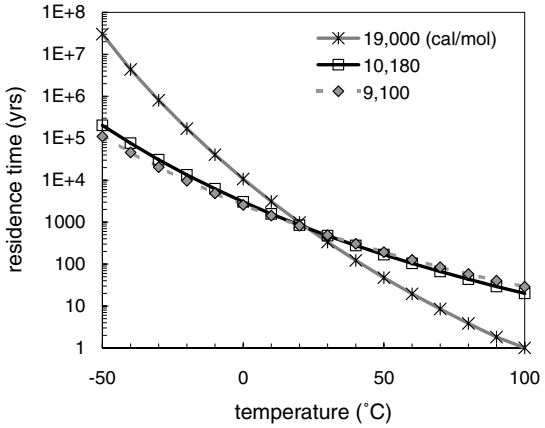

Fig. 3. Effect of activation energy on residence time calculations as a function of temperature. Activation energy values: 19,000 cal/mol (Wogelius and Walther, 1992), 10,180 cal/mol (Rosso and Rimstidt, 2000), and 9100 cal/mol (Grandstaff, 1986). At the highest and lowest temperatures, residence times (and dissolution rates) experience the largest dependence on activation energy.

there are several lines of evidence for acidic pH solutions on Mars (also discussed above). The exact pH is likely to be site-specific and will vary depending on local environmental factors. Temperature is more difficult to estimate, especially since it usually varies over time (daily, yearly, and longer periods of time). Knowing grain size is also important, and in site-specific determination of residence times, especially if microscopic images are available as they are for the Gusev site, the determination of accurate modal particle size should not be difficult. Regional and local particle sizes can also be determined remotely from thermal inertia values. The shergottite and nakhlite meteorites are samples of surface and near-surface lava flows, and their ages indicate that they represent only younger terrain. While the Martian meteorites do not represent the bulk of the Martian surface (e.g., Hamilton et al., 2003), the shergottites and nakhlites must have once been part of the surface but were more recently eroded or covered by dust and other deposits. Modal particle sizes are available for Martian meteorites, and while not linked to a specific locale on Mars, meteorites theoretically represent a random sampling of part of the Martian surface.

6. Discussion

Comparison of the estimated minimum residence times of olivine particles to the hypothetical durations of various Martian aqueous processes provides a method of evaluating the likelihood of olivine survival in each situation. It is important to keep in mind that times calculated by our

Table 4
Sensitivity analysis[f] of temperature effects for an olivine particle (Fo_{65}) at pH 4 with radius = 0.1 cm

Estimated T[a]	"Actual" T[b]	Calculated residence time[c] (yrs)	Δ Residence time[d] (yrs)	Coefficient[e] (γ_2)
25 °C (Calculated residence time 632 yrs)	5	6336	5704	0.10
	15	1922	1290	0.33
	20	1091	459	0.58
	30	372	−305	1.70
	35	223	−409	2.83
	50	53	−579	11.92

[a] The assumed or estimated temperature. An estimated temperature of 25 °C has a calculated residence time of 632 years under the given conditions.
[b] The hypothetical "actual" temperature (e.g., at a specific locale).
[c] The residence times (years) calculated at each "actual" temperature. When the "actual" temperature differs from the estimated temperature, the calculated residence time will be accordingly longer or shorter than the residence time at the estimated temperature of 25 °C (632 years at 25 °C under the given conditions).
[d] Δ residence time (years) is the difference between the calculated residence time at 25 °C (632 years) and the calculated residence time at the "actual" temperature.
[e] The coefficient (γ) is the calculated residence time at 25 °C divided by the calculated residence time at the "actual" temperature. For example, the difference (γ) in calculated residence times for the same particle at 5 °C and 25 °C under the given conditions is a factor of ~10.
[f] This table compares the calculated residence time for an assumed or estimated temperature with the residence times calculated for a range of hypothetical "actual" temperatures in order to show how uncertainty in temperature affects calculated residence times.

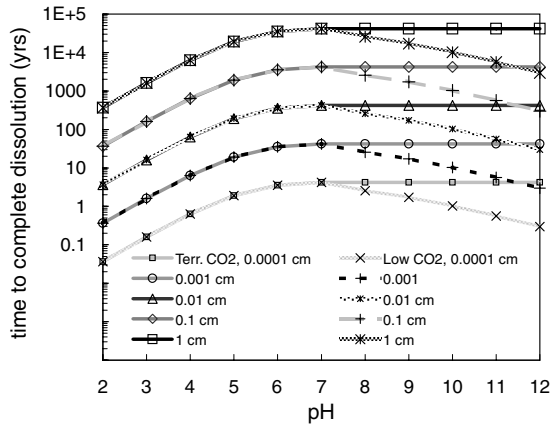

Fig. 4. Minimum time for complete dissolution of a single Fo_{65} particle at 25 °C. Time required depends on the particle radius (given in legend), P_{CO_2} (also given in legend, terrestrial (Terr.) $P_{CO_2} = 3.5 \times 10^{-4}$ bar, and low $P_{CO_2} \leqslant 3.2 \times 10^{-5\ \text{bar}}$), and pH.

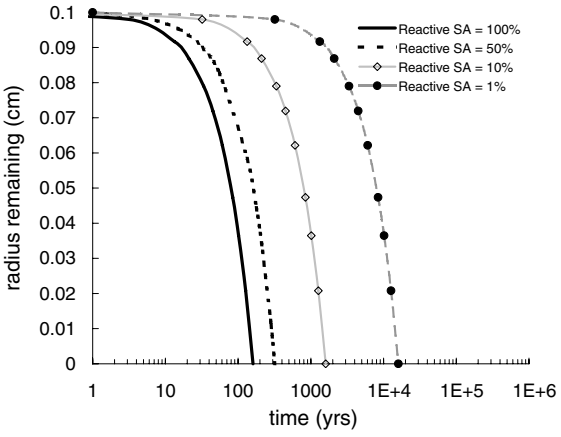

Fig. 5. Olivine residence times calculated for various reactive surface areas (100, 50, 10, and 1% of total surface area). Residence times are calculated for Fo_{65} olivine (radius = 0.1 cm) at pH 3 and 25 °C.

method will be minima, and actual times may be considerably longer (due to factors discussed above). Many aqueous processes are suggested to have occurred or be occurring on Mars, and the temporal duration of each is estimated in the literature (Table 5). Commonly cited low-temperature aqueous processes include outflow channel floods, valley network flows, gully formation, lakes, and oceans (e.g., Baker et al., 1991, 1992; McKay and Davis, 1991; Parker et al., 1993; Carr, 1996; Head et al., 1999; Malin and Edgett, 2000; Gulick, 2001; Kreslavsky and Head, 2002; Segura et al., 2002; Christensen, 2003). High-temperature hydrothermal systems can form due to impact heating or magmatic interactions (e.g., Gulick, 1998; Daubar and Kring, 2001; Abramov and Kring, 2005).

Fig. 6 compares calculated minimum residence times of Fo_{65} particles with radii 0.1 and 0.01 cm at 5 °C and pH 5 to the estimated duration of several low-temperature aqueous processes. Olivine is more likely to survive processes that fall near or below the plotted minimum residence times. Fo_{65} olivine particles at pH 5 (0.1 cm radii) can survive for ~20,000 years, and they may be able to survive short duration or intermittent, low-temperature aqueous processes such as melting ice or snow. However, long-lasting lakes and oceans can completely dissolve olivine particles of these (or smaller) sizes, except perhaps in the case of ultra-low temperature brines. Limited alteration of olivine is consistent with basalt dissolution experiments conducted by Baker et al. (2000) who concluded that the secondary mineral assemblages observed in most Martian meteorites are not consistent with long-term aqueous processes.

The dark solid line in Fig. 6 represents olivine dissolution under the least favorable conditions (not accounting for field vs. lab differences, which are discussed in Section 6.3 below). In Fig. 6, unfavorable dissolution conditions for a Fo_{65} particle are large size (0.1 cm radius), ultra-low temperature brine solution (−50 °C), and neutral pH. In this case, olivine particles might last over 200 Myr in a briny lake or ocean environment. For contrast, the speckled grey line in Fig. 6 represents olivine dissolution under more favorable conditions: small radius (0.01 cm), pH 2, and 25 °C. In this case, dissolution is much faster and olivine particles may survive only a few years in aqueous environments. At high (100 °C) temperatures, olivine particles can completely dissolve in a few years (Fig. 7). Thus, olivine is not likely to survive prolonged high-temperature hydrothermal activity, which may last 10,000 years or more (Gulick, 1998; Daubar and Kring, 2001).

Actual residence times may be somewhat longer than those calculated here due to surface coatings, saturated aqueous fluids, or changes in dissolution environment. Furthermore, quantification of the difference between experimental dissolution rates and those occurring in the field is difficult, and reactions in natural settings may proceed much more slowly than laboratory experiments suggest (e.g., Casey et al., 1993; White and Brantley, 2003). These potential factors are discussed below.

It is also important to remember that the residence times calculated here are for individual (or disconnected) spherical particles with ample fluid flow around all geometric surface area. These residence times do not represent olivine dissolution from basaltic rock. In the case of olivine dissolving from a rock matrix, rates will depend on porosity and permeability of the rock—both of which affect the accessibility of minerals to water. Cracks can greatly increase the permeability of bedrock. On Mars, much of the surface has probably experienced extensive impact events, forming a thick and fractured megaregolith (Hartmann et al., 2001). In unfractured rock, permeability is dominated by pore space and interconnectivity of voids (e.g., volcanic vesicles). If pore spaces and cracks can remain relatively free of precipitates and are large enough to allow ample fluid flow such that solutions do not become saturated, then these voids become transport channels for the products of dissolution. The rate at which the olivine in a rock matrix will dissolve depends on how much of the mineral surface area is in contact with unsaturated

Table 5
Possible timescales of aqueous processes on Mars

Aqueous process	Duration
Low T:	
Outflow channels formed by periodic flooding through catastrophic release of water	Short-lived, <1 yr[a] over a period of several months[b]
Valley networks formed by release of groundwater during impact	Few 100 years[c] over a period of several 100,000 years[d]
Gullies formed by melting snow	~5,000 years[e]
Lakes and lacustrine deposition	Up to several 100 million years[a]
Oceans and marine deposition	10,000-billions of years[f,g,h]
High T:	
Hydrothermal activity from impact	10,000–10 million years[i,j]
Hydrothermal activity from magmatic interactions	Few 100,000 years or more[k]

[a] Carr (1996).
[b] Baker et al. (1991).
[c] Segura et al. (2002).
[d] Gulick (2001).
[e] Christensen (2003).
[f] Kreslavsky and Head (2002).
[g] McKay and Davis (1991).
[h] Parker et al. (1993).
[i] Daubar and Kring (2001).
[j] Abramov and Kring (2005).
[k] Gulick (1998).

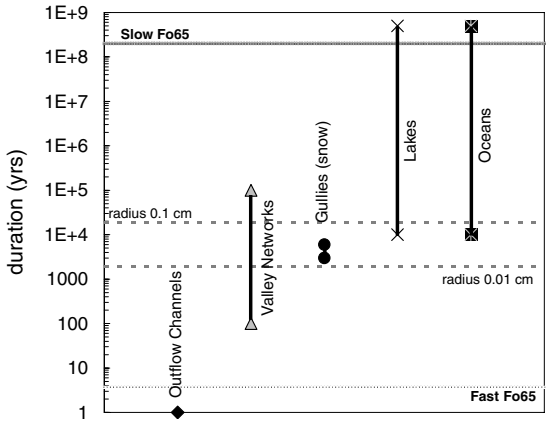

Fig. 6. Estimated duration of low temperature aqueous processes on Mars (for references see Table 1 caption) compared to calculated minimum residence times of a Fo_{65} particle at 5 °C and pH 5. An olivine particle with radius 0.01 cm will endure for ~2,000 years under these conditions (lower dashed line), and a particle with radius 0.1 cm will endure for ~20,000 years (upper dashed line). Olivine might survive processes that fall near or below the dashed lines (minimum residence times for Fo_{65} at 5 °C at different particle sizes). However, long-lasting lakes and oceans can completely weather olivine particles except perhaps in the case of ultra-low temperature brines. The grey line "Slow Fo_{65}" at ~200 Myr represents olivine dissolution under the least favorable conditions (not accounting for field vs. lab differences), which is a brine at −50 °C, radius = 0.1 cm, and pH 7. The grey line "Fast Fo_{65}" at ~4 years represents olivine dissolution under the most favorable conditions: radius = 0.01 cm, pH 2, and 25 °C.

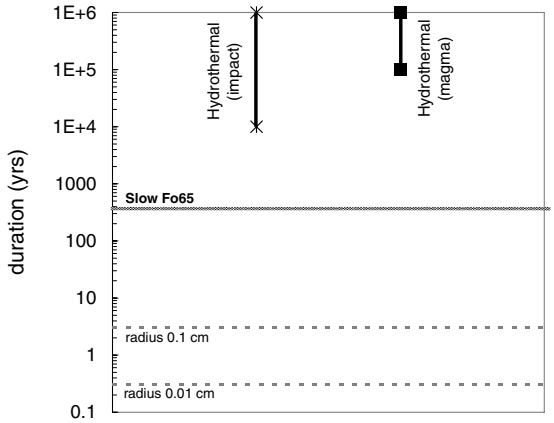

Fig. 7. Estimated duration of high temperature aqueous processes on Mars (for references see Table 1 caption) compared to calculated minimum residence times of a Fo_{65} olivine particle at 100 °C and pH 5. An olivine particle with radius 0.01 cm will endure for ~0.3 years under these conditions (lower dashed line), and a particle with radius 0.1 cm will endure for ~3 years (upper dashed line). The grey line "Slow Fo_{65}" at ~368 years represents olivine dissolution under the least favorable (high temperature) conditions (not accounting for field vs. lab differences), which are 100 °C, radius = 0.1 cm, and pH 7. Due to the very quick dissolution rates of olivine at high temperatures, particles are unlikely to survive hydrothermal processes.

solutions. The effects of reduced reactive surface area may increase residence times by approximately a factor of 10 (discussed above), and increased saturation in transport-limited regimes such as small cracks or pore spaces in rock matrix (discussed below in Section 6.2) may only increase residence times by a factor of 3.3. Therefore, even olivine in bedrock can dissolve under the right conditions, and it may take only a factor of 33 times longer than the dissolution of isolated olivine particles (such as sand). The depth and extent of subsurface dissolution will depend on how deeply water can penetrate and how well ions can be transported out of the rock. More connectivity and larger voids allow better access to minerals at depth and help prevent solution saturation. At the surface-rock interface, if mechanical weathering can loosen olivine grains from the rock matrix, then water will more readily react with the entire surface area, leaving olivine more susceptible to disso-

lution. Fine particulate material created by mechanical erosion can be either altered in situ or transported and deposited elsewhere (where it may experience different environmental conditions). In situ dissolution of fine, eroded olivine particles will proceed more rapidly than for olivine grains within the host rock.

6.1. Effect of oxidation, P_{O_2}, and surface coatings

We have largely ignored the formation of secondary phases on mineral surfaces (or on the surface of the host-rock). It is possible that the formation of coatings on rock and mineral surfaces can prevent dissolution by prohibiting the access of water to olivine grains, and these coatings may persist until geochemical instability or mechanical erosion can remove (or bypass) them. Oxidation due to the presence of atmospheric O_2 can lead to the formation of such surface coatings on fayalitic olivine particles, thus reducing the rate of olivine dissolution over time. However, Wogelius and Walther (1992) estimate that terrestrial rates of olivine oxidation are ~2 orders of magnitude slower than dissolution rates; therefore, under favorable conditions olivine dissolution should outpace oxidation and the formation of surface coatings. In studies of forsterite dissolution, Tosca et al. (2004) did not observe the formation of any surface coatings. Thus, the extent of surface coatings on olivine may be a function of Fe^{2+} availability as well as P_{O_2}. Oxidation has also been observed to vary with pH. For example, Santelli et al. (2001) observed faster oxidation at pH 3 than at pH 2.

While P_{O_2} on Mars is relatively low (especially compared to that on the earth), the surface is notorious for its red, oxidized color. Nonetheless, based solely on the P_{O_2} of Mars, we would infer that oxidation should not have as large of an effect on surface/subsurface dissolution reactions as it does on Earth. Burns (1993), who considered P_{O_2}, temperature, pH, and ionic strength of solution, calculated that oxidation rates should be several orders of magnitude lower on Mars than on Earth, which implies that dissolution on Mars should proceed virtually unhindered by oxidized surface coatings.

6.2. Effect of cations in solution and saturation

As a mineral dissolves, it will increase the local concentration of aqueous species, especially in transport-limited regimes. In our model, we did not consider the effects of changing solution chemistry over time. However, an increase in the concentration of aqueous species can decrease the dissolution of some minerals (Sak et al., 2004). In general, dissolution of olivine appears to be independent of dissolved species such as Mg^{2+}, Fe^{2+}, Al^{3+}, and silica (Chen and Brantley, 2000; Oelkers, 2001a; Santelli et al., 2001). However, Pokrovsky and Schott (2000b) observed changes in the dissolution rate of olivine as a function of aqueous silica concentration at high pH. Conversely, studies thus far have not shown a correlation between olivine dissolution and concentration of dissolved species in acidic solutions (Chen and Brantley, 2000; Oelkers, 2001a; Santelli et al., 2001), which is the pH-regime most relevant to Mars.

The saturation state of aqueous solutions can also affect dissolution, and natural solutions are typically closer to equilibrium than laboratory solutions (Brantley, 2003). It is generally agreed that the abundance of etch pits decreases as solutions near equilibrium (e.g., Sak et al., 2004). Etch pits are one potential site where dissolution may begin, and their evolution also depends on saturation state. Lasaga and Luttge (2001) observed the formation of globally-advancing "stepwaves" that emanate from etch pits at far-from-equilibrium conditions. When the solution is more saturated (and closer to equilibrium) dissolution is slower because these stepwaves do not form. Dissolution rates decrease non-linearly as solutions become less dilute and move toward saturation, and even if rates are reduced by 70%, calculated residence times for olivine are increased only by a factor of ~3.3. If dissolution rates are reduced by 90%, calculated residence times are only increased by a factor of 10 (Table 6).

6.3. Experimental vs. field rates

It is difficult to account for all natural variables in a laboratory setting; therefore, differences between experimental and field dissolution rates should be expected. However, White and Brantley (2003) report that the differences may be between two and four orders of magnitude. One important difference between laboratory and field rates is the length of time over which the material has experienced alteration. In the lab, experiments are usually conducted on short time scales (hours to years), whereas in the field, rocks and minerals have been exposed to the elements much longer (years to millions of years). Furthermore, natural environments are likely to change with time, and aqueous solutions may be present only intermittently. Cycles of wet and dry periods are generally thought to decrease surface reactions due to several factors: formation of secondary phases, condensation of species onto mineral surfaces, or saturation of solution (Blum and Stillings, 1995; White and Brantley, 2003).

White and Brantley (2003) observed a decrease in dissolution rates of various silicate minerals (olivine was not studied) over a period of several years in a laboratory environment. They suggest that dissolution rate constants (mol cm^{-2} s^{-1}) may decrease as a power function of time (seconds):

$$R_{\text{silicate}} = 3.1 \times 10^{-17}(t^{-0.61}) \quad (9)$$

Part of this difference may be due to a decrease in surface defects on grains with time or normalization to BET-calculated surface area. Lasaga and Luttge (2001) proposed that slower dissolution in more saturated solutions may explain part of the difference between lab and field rates, because in natural environments, solutions tend toward equilibrium conditions and, therefore, dissolution rates are likely to be slower. Fig. 8

Table 6
Effect of near-equilibrium conditions on olivine dissolution rates and residence times, calculated for Fo_{65} olivine at 25 °C

pH	Dissolution rate (mol cm^{-2} s^{-1})	Rate reduction (%)	Reduced rate	Time to complete dissolution (yrs)
3 (radius 0.01 cm)	4.84×10^{-13}	0	4.84×10^{-13}	16
		10	4.36×10^{-13}	18
		20	3.87×10^{-13}	20
		30	3.39×10^{-13}	23
		40	2.9×10^{-13}	27
		50	2.42×10^{-13}	32
		60	1.94×10^{-13}	40
		70	1.45×10^{-13}	53
		80	9.68×10^{-14}	80
		90	4.84×10^{-14}	160
5 (radius 0.1 cm)	4.06×10^{-14}	0	4.06×10^{-14}	1900
		10	3.66×10^{-14}	2100
		20	3.25×10^{-14}	2400
		30	2.85×10^{-14}	2700
		40	2.44×10^{-14}	3200
		50	2.03×10^{-14}	3800
		60	1.63×10^{-14}	4800
		70	1.22×10^{-14}	6400
		80	8.13×10^{-15}	9500
		90	4.06×10^{-15}	19,000

illustrates the difference in residence time between an olivine particle in our model, and a generalized silicate particle following the average silicate time-dependent rate expression (from White and Brantley, 2003). Much of this difference is due to the overall slower dissolution of other silicates compared to olivine. In a simpler approach, we apply a 10^2–10^4 correction factor in the following sections as an estimate of how much longer our modeled dissolution would take in a natural environment on Mars. This approach tries to account for changing pH, solution composition, decreasing dissolution rates with time, as well as other natural processes that might slow dissolution rates on Mars, and it also provides an upper limit on residence times to compliment our calculated minimum times.

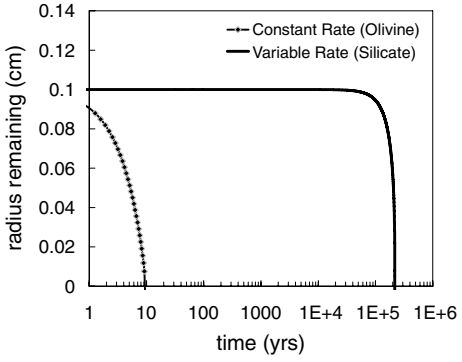

Fig. 8. Residence time of a mineral following the average silicate time-dependent expression for dissolution rate (from White and Brantley, 2003) compared to olivine at pH 3 and 25 °C. Particle size of both minerals is assumed to be 0.1 cm (radius). Much of the difference in residence times is due to the overall slower rate of silicates in general compared to olivine.

6.4. Early Mars and maximum residence times

The numerous morphological features resembling fluvially carved valleys and channels suggest that liquids must have once flowed over the surface of Mars. It is possible that different climatic conditions once existed such as a "warm, wet" Mars (e.g., Pollack et al., 1987), a time when long-term temperatures were warmer (above 0 °C). How would a fairly large, though not unlikely size for Martian olivine, 0.5 mm (radius) olivine (Fo_{65}) particle fare in such an environment ($T = 5$ °C) at pH 7, where dissolution rates are slowest? Strictly following the rate equations outlined above, such a particle would last at least 2100 years. As a rough estimate of the maximum residence time of such a particle, we multiply our calculated minimum residence time by 10^2 and 10^4, assuming that this correction factor will account for all differences between lab and field rates. After the correction factor is applied, we estimate a maximum residence time of olivine on a "warm, wet" Mars to be ~210,000 to 21 Myr. If pH is acidic (pH 3 instead of neutral as assumed in this example) olivine particles should dissolve more readily and maximum residence times will be even shorter (~8000–800,000 years). If we assume brine-free conditions, then temperatures must be >0 °C in order for chemical reactions with water to occur. If temperatures were higher than 5 °C, then olivine will dissolve faster and maximum residence times will again be shortened. If olivine was more iron-rich, as seen in various Martian meteorites, maximum residence times would be further reduced. Taking all of these factors into account, the kinetics of olivine dissolution suggest that if an early "warm, wet" period did occur, olivine present in the basaltic crust at the time would not survive long-term in the presence of liquid water: ~21 Myr in the worst-case scenario, which is much

less than the duration of the putative early "warm, wet" Mars. However, olivine may survive longer if dissolution is inhibited, for example, during long intermittent dry periods.

Although we cannot date the TES olivine-rich areas using geochemical models, Hoefen et al. (2003) bounded the upper limit of olivine exposure in the Nili Fossae region to be 3.8-3.6 Ga based on the crater counts of Hiesinger and Head (2002). If indeed the olivine-rich surface in the Nili Fossae region is billions of years old, then our ~21 Myr maximum residence time and minimum residence times on the order of a few years suggest that the olivine has only had brief or intermittent exposure to aqueous solutions and that the climate in this region has been either too cold or too dry to allow significant olivine dissolution over most of its history. Based on studies of thermal inertia, Hamilton and Christensen (2005) have suggested that much of the olivine in this region is in the form of bedrock overlain by varying amounts of finer particles. In bedrock, olivine exposure to liquids can be prohibited by protective coatings, very low porosity, and/or very low permeability of the rocks. Also, physical erosion, if proceeding at a rate greater than aqueous alteration, might continuously expose fresh olivine-bearing rocks at the surface. However, the finer eroded material should dissolve quickly if exposed to aqueous solution.

If early olivine is more magnesian (Fo_{91}) as suggested by Koeppen and Hamilton (2006), then the maximum residence time of a 0.5 mm (radius) olivine particles at 5 °C and pH 7 is ~380,000 to 38 Myr. Further investigation is required to explain the observed correlation between olivine iron content and surface age. However, if mantle evolution and igneous processes cannot alone account for this correlation, then the kinetics of olivine dissolution can offer several hypotheses to explain the observation. First, Mg-rich olivine dissolves approximately 10 times slower than fayalite and may resist dissolution longer under hydrated conditions. Thus, it may be possible that Fe-rich olivine grains have been selectively removed by dissolution during a wet clime that did not persist long enough to remove the magnesian olivine grains. Alternatively, Fe-rich olivine rims are more susceptible to dissolution than Mg-rich cores, which might survive longer in aqueous conditions, thereby explaining the observed olivine trend as the survival of Mg-rich cores but the dissolution of Fe-rich rims. A third possibility is that iron is selectively removed in solution without much loss of surface area, as seen in the nakhlite MIL 03346 (Stopar et al., 2005) where olivine veins are enriched in Fe while olivine along the veins has lost Fe. In this scenario, older olivine has undergone more alteration because it has experienced more hydration events and has lost more of its iron.

6.5. Recent Mars

Gusev Crater, formed in the Noachian, was selected as a MER landing site chosen for its potential lacustrine deposits (e.g., Grant et al., 2004; Squyres et al., 2004a). However, younger basalts (3.65 Ga) appear to have invaded the crater (Greeley et al., 2005) and no unequivocal evidence remains available for the Spirit Rover to indicate the presence of ancient aqueous sedimentation (Squyres et al., 2004a). There is, however, definitive evidence for more recent aqueous alteration of rocks and soils at Gusev Crater (Haskin et al., 2005) where olivine is found as fine grains in the soil as well as in surface rocks. The presence of veins and filled voids in the interior of some basaltic surface rocks suggests some aqueous processes have occurred. However, the overall unaltered nature of olivine in the fine soil and in rocks suggests that little dissolution has occurred since deposition of the basaltic rocks. According to kinetic models, fine particles, such as those in the soil, with diameters <0.5 mm will dissolve quickly (few thousand years) in dilute aqueous solutions at 5 °C and slightly acidic pH. The survival of these tiny olivine particles suggests that the availability of liquid water at the Gusev site has been very limited since the deposition of the basaltic soil component.

Meridiani Planum was selected as a MER landing site (Squyres et al., 2004b) because of the unusual coarse-grained hematite signature observed in orbital thermal IR spectra (Christensen et al., 2000b, 2001). At Meridiani there is chemical evidence from the Alpha-Proton X-ray Spectrometer (APXS) for silicate dissolution (presumably olivine) of the original basaltic surface (Rieder et al., 2004) and deposition of sulfates and chemically-altered sediments in water during episodic inundation events (Squyres et al., 2004b). The fluid from which the evaporites have precipitated is thought to be composed of ions derived from olivine-bearing basalts (McLennan et al., 2005). However, since the formation of the sulfur-rich bedrock, little chemical alteration has occurred. There has been some cementation of sand grains (Squyres et al., 2004b), but since the deposition of the olivine-bearing basaltic sands, physical weathering and aeolian transport of basaltic materials has prevailed (Christensen et al., 2004b). Chemical data (APXS) indicate that there is a weathering profile in the soils at both MER landing sites where olivine, Fe^{2+}, and Br concentration increase while S, Cl, and Fe^{3+} concentration decrease with depth in the soil (Yen et al., 2005). The presence of olivine at depth in the soils suggests that little alteration has occurred. Yen et al. (2005) hypothesize that ephemeral, reoccurring, thin films of liquid water could condense from the atmosphere and, given enough time, alter the upper soil layers to create the observed weathering gradient. The finest fraction of olivine particles ~0.1 mm in diameter (Herkenhoff et al., 2004b) would certainly dissolve extremely fast under favorable conditions. A Fo_{65} particle 0.1 mm in diameter can completely dissolve in ~80 years in dilute solutions of pH 3 (calculated at 25 °C). Even if dissolution rates are 10^3 times slower due to solution saturation, low water/rock ratio, or decreased reactive surface area, the same particle would completely dissolve in 80,000 years, suggesting that the basaltic sands on the Meridiani surface have had limited exposure to liquid water.

7. Summary and conclusions

We have calculated minimum residence times, and our calculations show that when dissolution progresses at its fullest capacity olivine particles can completely dissolve within a few years. The most favorable conditions for olivine dissolution are fayalite-rich compositions, small particle sizes (e.g., $\leqslant$1 mm radius), high temperatures (e.g., >25 °C), and acidic solutions (e.g., pH <3) that are far from equilibrium. The least favorable conditions for olivine dissolution are forsterite-rich compositions, large particle sizes (e.g., >1 cm radius), ultra-low temperatures (e.g., <0 °C), and a neutral pH solution that is near equilibrium.

By bounding dissolution rates and residence times, we can make inferences about the temporal extent of aqueous alteration on the surface of Mars. Hypothesized aqueous processes were compared to the calculated duration of 0.1 and 0.01 cm (radius) olivine particles under various conditions (Figs. 6 and 7). Our results confirm that dissolution times for olivine are generally rapid and that fayalitic particles dissolve ~10 times faster than forsteritic ones. At standard temperature (25 °C), the residence time of a 0.1 cm (radius) particle of Fo_{65} composition ranges from ~37 years at pH 2 to ~4200 years at pH 7. At lower temperature (5 °C), dissolution of the same particle will take ~10 times longer.

While we have focused on minimum residence times, an estimate of maximum residence times can be made by assuming a factor of 10^2–10^4 difference between minimum residence times and maximum residence times. Fo_{65} olivine particles at 5 °C and pH 7 with 0.5 mm radii, have a tentative maximum residence time of ~21 Myr, and Fo_{91} particles of the same size and under the same conditions have a tentative maximum residence time of ~38 Myr. However, care should be taken when using this maximum estimate as many of the underlying factors involved in the 10^2 and 10^4 modifications are poorly constrained at present.

This work is a first step in constraining olivine dissolution rates on Mars. In spite of all the complications and uncertainties involved in extrapolating experimental mineral rates to another planet, it is apparent that olivine is generally not stable in contact with aqueous fluids over geologic time periods, with the possible exception of briny solutions at ultra-low temperatures and solutions at or very near equilibrium. The survival of olivine on the surface of Mars (especially in older terrains) implies that contact with aqueous solutions has been limited.

Acknowledgments

The authors thank K. Ruttenburg, P. G. Lucey, and F. S. Anderson (University of Hawaii) for their constructive suggestions and reviews of this material during its early development. We also thank Clive R. Neal (Associate editor), Scott McLennan, and an anonymous reviewer for their helpful and insightful comments during review for publication. This material is based upon work partly supported by the National Aeronautics and Space Administration through the NASA Astrobiology Institute under Cooperative Agreement No. NNA04CC08A issued through the Office of Space Science. This work was supported by NASA (contract #JPL1241588), the University of Arizona (contract #Y402065), and a NASA Graduate Student Researchers Program (GSRP) fellowship.

Associate editor: Clive R. Neal

References

Abramov, O., Kring, D.A., 2005. Impact-induced hydrothermal activity on early Mars. *J. Geophys. Res.* **110**. doi:10.1029/2005JE002453.

Andersen, D.T., Pollard, W.H., McKay, C.P., Heldmann, J., 2002. Cold springs in permafrost on Earth and Mars. *J. Geophys. Res.* **107**. doi:10.1029/2000JE001436.

Baker, L.L., Agenbroad, D.J., Wood, S.A., 2000. Experimental hydrothermal alteration of a Martian analog basalt: implications for Martian meteorites. *Meteorit. Planet. Sci.* **35**, 31–38.

Baker, V.R., Strom, R.G., Gulick, V.C., Kargel, J.S., Komatsu, G., Kale, V.S., 1991. Ancient oceans, ice sheets and the hydrological cycle on Mars. *Nature* **352**, 589–594.

Baker, V.R., Marley, M.S., Carr, M.H., Gulick, V.C., Williams, C.R., 1992. Channels and valley networks. In: Kieffer, H.H., Jakosky, B.M., Snyder, C.W., Matthews, M.S. (Eds.), *Mars*. The University of Arizona Press, Tucson, pp. 493–522.

Bandfield, J.L., Hamilton, V.E., Christensen, P.R., 2000. A global view of Martian surface compositions from MGS-TES. *Science* **287**, 1626–1630.

Banin, A., Clark, B.C., Wanke, H., 1992. Surface chemistry and mineralogy. In: *Mars*. Arizona University Press, Tucson, pp. 594–625.

Beck, P., Barrat, J.A., Gillet, P., Wadhwa, M., Franchi, I.A., Greenwood, R.C., Bohn, M., Cotton, J., van de Moortele, B., Reynard, B., 2006. Petrography and geochemistry of the chassignite Northwest Africa 2737 (NWA 2737). *Geochim. Cosmochim. Acta* **70**, 2127–2139.

Blum, A.E., Stillings, L.L., 1995. Feldspar dissolution kinetics. In: *Chemical Weathering Rates of Silicate Minerals*. In: White, A.F., Brantley, S.L. (Eds.), *Reviews in Mineralogy*, Vol. 31. Mineralogical Society of America, Washington DC, pp. 291–351.

Boynton, W.V., Feldman, W.C., Squyres, S.W., Prettyman, T.H., Bruckner, J., Evans, L.G., Reedy, R.C., Starr, R., Arnold, J.R., Drake, D.M., Englert, P.A.J., Metzger, A.E., Mitrofanov, I., Trombka, J.I., d'Uston, C., Wanke, H., Gasnault, O., Hamara, D.K., Janes, D.M., Marcialis, R.L., Maurice, S., Mikheeva, I., Taylor, G.J., Tokar, R., Shinohara, C., 2002. Distribution of hydrogen in the near surface of Mars: evidence for subsurface ice deposits. *Science* **297**, 81–85.

Brantley, S.L., 2003. Reaction kinetics of primary rock-forming minerals under ambient conditions. In: Drever, J.I. (Ed.), *Treatise on Geochemistry*, vol. 5. Elsevier, Amsterdam, pp. 73–117.

Burns, R.G., 1993. Rates and mechanisms of chemical weathering of ferromagnesian silicate minerals on Mars. *Geochim. Cosmochim. Acta* **37**, 4555–4574.

Burt, D.M., Knauth, L.P., 2003. Electrically conducting, Ca-rich brines, rather than water, expected in the Martian subsurface. *J. Geophys. Res.* **108**. doi:10.1029/2002JE001862.

Carr, M.H., 1996. *Water on Mars*. Oxford University Press, New York, 229 p.

Casey, W.H., Banfield, J.F., Westrich, H.R., McLaughlin, L., 1993. What do dissolution experiments tell us about natural weathering? *Chem. Geol.* **105**, 1–15.

Chen, Y., Brantley, S.L., 2000. Dissolution of forsteritic olivine at 65 °C and 2 < pH < 5. *Chem. Geol.* **165**, 267–281.

Christensen, P.R., 2003. Formation of recent Martian gullies through melting of extensive water-rich snow deposits. *Nature* **422**, 45–47.

Christensen, P.R., Bandfield, J.L., Smith, M.D., Hamilton, V.E., Clark, R.N., 2000a. Identification of a basaltic component on the Martian surface from thermal emission spectrometer data. *J. Geophys. Res.* **105**, 9609–9621.

Christensen, P.R., Bandfield, J.L., Clark, R.N., Edgett, K.S., Hamilton, V.E., Hoefen, T., Kieffer, H.H., Kuzmin, R.O., Lane, M.D., Malin, M.C., Morris, R.V., Pearl, J.C., Pearson, R., Roush, T.L., Ruff, S.W., Smith, M.D., 2000b. Detection of crystalline hematite mineralization on Mars by the thermal emission spectrometer: evidence for near-surface water. *J. Geophys. Res.* **105**, 9623–9642.

Christensen, P.R., Morris, R.V., Lane, M.D., Bandfield, J.L., Malin, M.C., 2001. Global mapping of Martian hematite mineral deposits: remnants of water-driven processes on early Mars. *J. Geophys. Res.* **106**, 23873–23885.

Christensen, P.R., Ruff, S.W., Fergason, R.L., Knudson, A.T., Anwar, S., Arvidson, R.E., Bandfield, J.L., Blaney, D.L., Budney, C., Calvin, W.M., Glotch, T.D., Golombek, M.P., Gorelick, N., Graff, T., Hamilton, V.E., Hayes, A.G., Johnson, J.R., McSween Jr., H.Y., Mehall, G.L., Mehall, L.K., Moersch, J.E., Morris, R.V., Rogers, A.D., Smith, M.D., Squyres, S.W., Wolff, M.J., Wyatt, M.B., 2004a. Initial results from the Mini-TES experiment in Gusev Crater from the Spirit Rover. *Science* **305**, 837–842.

Christensen, P.R., Wyatt, M.B., Glotch, T.D., Rogers, A.D., Anwar, S., Arvidson, R.E., Bandfield, J.L., Blaney, D.L., Budney, C., Calvin, W.M., Fallacaro, A., Fergason, R.L., Gorelick, N., Graff, T.G., Hamilton, V.E., Hayes, A.G., Johnson, J.R., Knudson, A.T., McSween Jr., H.Y., Mehall, G.L., Moersch, J.E., Morris, R.V., Smith, M.D., Squyres, S.W., Ruff, S.W., Wolff, M.J., 2004b. Mineralogy at Meridiani Planum from the Mini-TES experiment on the Opportunity rover. *Science* **306**, 1733–1739.

Daubar, I.J., Kring, D.A., 2001. Impact-induced hydrothermal systems: heat sources and lifetimes. Lunar and Planetary Science Conference XXXII, Abstract #1727.

Deer, W.A., Howie, R.A., Zussman, J., 1992. Olivine Group. In: *An Introduction to the Rock Forming Minerals*, second ed. Longman, Harlow, England, pp. 3–13.

Eggleton, R.A., 1986. The relation between crystal structure and silicate weathering rates. In: Colman, S.M., Dethier, D.P. (Eds.), *Rates of Chemical Weathering of Rocks and Minerals*. Academic Press, Inc., Orlando, Florida, pp. 21–42.

Goodrich, C.A., 2002. Olivine-phyric Martian basalts: a new type of shergottite. *Meteorit. Planet. Sci.* **37** (Supplement), B31–B34.

Grandstaff, D.E., 1986. The dissolution rate of forsteritic olivine from Hawaiian beach sand. In: Colman, S.M., Dethier, D.P. (Eds.), *Rates of Chemical Weathering of Rocks and Minerals*. Academic Press, Inc., Orlando, Florida, pp. 41–59.

Grant, J.A., Arvidson, R.E., Bell III, J.F., Cabrol, N.A., Carr, M.H., Christensen, P.R., Crumpler, L.S., Des Marais, D.J., Ehlmann, B.L., Farmer, J.D., Golombek, M.P., Grant, F.D., Greeley, R., Herkenhoff, K.E., Li, R., McSween Jr., H.Y., Ming, D.W., Moersch, J.E., Rice Jr., J.W., Ruff, S.W., Richter, L., Squyres, S.W., Sullivan, R., Weitz, C., 2004. Surficial deposits at Gusev Crater along Spirit Rover traverses. *Science* **305**, 807–810.

Greeley, R., Fiong, B.H., McSween Jr., H.Y., Neukum, G., Pinet, P., van Kan, M., Werner, S.C., Williams, D.A., Zegers, T.E., 2005. Fluid lava flows in Gusev crater, Mars. *J. Geophys. Res.* **110**. doi:10.1029/2005JE002401.

Gulick, V.C., 1998. Magmatic intrusions and a hydrothermal origin for fluvial valleys on Mars. *J. Geophys. Res.* **103**, 19365–19387.

Gulick, V.C., 2001. Origin of the valley networks on Mars: a hydrological perspective. *Geomorphology* **37**, 241–268.

Hamilton, V.E., Christensen, P.R., 2003. Detailed mineralogical analyses of Martian meteorite-like terrains using MGS TES and Odyssey THEMIS data. Lunar and Planetary Science Conference XXXIV, Abstract #1982.

Hamilton, V.E., Christensen, P.R., 2004. Green Mars: geologic characteristics of olivine-bearing terrains as observed by THEMIS, MOC, and MOLA. Lunar and Planetary Science Conference XXXV, Abstract #2131.

Hamilton, V.E., Christensen, P.R., 2005. Evidence for extensive, olivine-rich bedrock on Mars. *Geology* **33**, 433–436.

Hamilton, V.E., Christensen, P.R., McSween Jr., H.Y., Bandfield, J.L., 2003. Searching for the source regions of Martian meteorites using MGS TES: Integrating Martian meteorites into the global distribution of igneous materials on Mars. *Meteorit. Planet. Sci.* **38**, 871–885.

Hartmann, W.K., Anguita, J., de La Casa, M.A., Berman, D.C., Ryan, E.V., 2001. Martian cratering 7: The role of impact gardening. *Icarus* **149**, 37–53.

Haskin, L.A., Wang, A., Jolliff, B.L., McSween Jr., H.Y., Clark, B.C., Des Marais, D.J., McLennan, S.M., Tosca, N.J., Hurowitz, J.A., Farmer, J.D., Yen, A., Squyres, S.W., Arvidson, R.E., Klingelhofer, G., Schroder, C., de Souza Jr., P.A., Ming, D.W., Gellert, R., Zipfel, J., Bruckner, J., Bell III, J.F., Herkenhoff, K., Christensen, P.R., Ruff, S.W., Blaney, D.L., Gorevan, S., Cabrol, N., Crumpler, L., Grant, J.A., Soderblom, L., 2005. Water alteration of rocks and soils on Mars at the Spirit rover site in Gusev crater. *Nature* **436**, 66–69.

Head III, J.W., Hiesinger, H., Ivanov, M.A., Kreslavsky, M.A., Pratt, S., Thomson, B.J., 1999. Possible ancient oceans on Mars: Evidence from Mars Orbiter Laser Altimeter data. *Science* **286**, 2134–2137.

Herkenhoff, K.E., Squyres, S.W., Arvidson, R.E., Bass, D.S., Bell III, J.F., Bertelsen, P., Cabrol, N.A., Gaddis, L., Hayes, A.G., Hviid, S.F., Johnson, J.R., Kinch, K.M., Madsen, M.B., Maki, J.N., McLennan, S.M., McSween Jr., H.Y., Rice Jr., J.W., Sims, M., Smith, P.H., Soderblom, L.A., Spanovich, N., Sullivan, R., Wang, A., 2004a. Textures of the soils and rocks at Gusev Crater from Spirit's Microscopic Imager. *Science* **305**, 824–826.

Herkenhoff, K.E., Squyres, S.W., Arvidson, R.E., Bass, D.S., Bell III, J.F., Bertelsen, P., Ehlmann, B.L., Farrand, W.H., Gaddis, L., Greeley, R., Grotzinger, J.P., Hayes, A.G., Hviid, S.F., Johnson, J.R., Jolliff, B.L., Kinch, K.M., Knoll, A.H., Madsen, M.B., Maki, J.N., McLennan, S.M., McSween Jr., H.Y., Ming, D.W., Rice Jr., J.W., Richter, L., Sims, M., Smith, P.H., Soderblom, L.A., Spanovich, N., Sullivan, R., Thompson, S., Wdowiak, T., Weitz, C., Whelley, P., 2004b. Evidence from Opportunity's Microscopic Imager for water on Meridiani Planum. *Science* **306**, 1727–1730.

Hiesinger, H., Head III, J.W., 2002. Syrtis Major, Mars: results from Mars Global Surveyor data. Lunar and Planetary Science Conference **XXXIII**, Abstract #1063.

Hoefen, T.M., Clark, R.N., 2001. Compositional variability of Martian olivines using Mars Global Surveyor thermal emission spectra. Lunar and Planetary Science Conference XXXII, Abstract #2049.

Hoefen, T.M., Clark, R.N., Bandfield, J.L., Smith, M.D., Pearl, J.C., Christensen, P.R., 2003. Discovery of olivine in the Nili Fossae region of Mars. *Science* **302**, 627–630.

Kieffer, H.H., Martin, T.Z., Peterfreund, A.R., Jakosky, B.M., 1977. Thermal and albedo mapping of Mars during the Viking primary mission. *J. Geophys. Res.* **82**, 4249–4291.

Klein, C., Hurlbut, C.S., 1993. Systematic Mineralogy Part IV: Silicates. In: *Manual of Mineralogy*, Twentyfirst ed. John Wiley and Sons, New York, pp. 440–557.

Klingelhofer, G., Morris, R.V., Bernhardt, B., Schroder, C., Rodionov, D.S., de Souza Jr., P.A., Yen, A., Gellert, R., Evlanov, E.N., Zubkov, B., Foh, J., Bonnes, U., Kankeleit, E., Gutlich, P., Ming, D.W., Renz, F., Wdowiak, T., Squyres, S.W., Arvidson, R.E., 2004. Jarosite and hematite at Meridiani Planum from Opportunity's Mossbauer Spectrometer. *Science* **306**, 1740–1745.

Koeppen, W.C., Hamilton, V.E., 2006. The distribution and composition of olivine on Mars. Lunar and Planetary Science Conference XXXVII, Abstract #1964.

Kreslavsky, M.A., Head III, J.W., 2002. Fate of outflow channel effluents in the northern lowlands of Mars: The Vastitas Borealis Formation as a sublimation residue from frozen ponded bodies of water. *J. Geophys. Res.* **107**. doi:10.1029/2001JE001831.

Langmuir, 1997. Iron-Sulfur Redox Chemistry. In: *Aqueous Environmental Geochemistry*. Prentice Hall, Upper Saddle River, New Jersey, pp. 431–485.

Lasaga, A.C., 1984. Chemical kinetics of water-rock interactions. *J. Geophys. Res.* **89**, 4009–4025.

Lasaga, A.C., Luttge, A., 2001. Variation of crystal dissolution rate based on a dissolution stepwave model. *Science* **291**, 2400–2404.

Lasaga, A.C., Soler, J.M., Ganor, J., Burch, T.E., Nagy, K.L., 1994. Chemical weathering rate laws and global geochemical cycles. *Geochim. Cosmochim. Acta* **58**, 2361–2386.

Malin, M.C., Edgett, K.S., 2000. Evidence for recent groundwater seepage and surface runoff on Mars. *Science* **288**, 2330–2335.

McKay, C.P., Davis, W.L., 1991. Duration of liquid water habitats on early Mars. *Icarus* **90**, 214–221.

McLennan, S.M., Bell III, J.F., Calvin, W.M., Christensen, P.R., Clark, B.C., de Souza Jr., P.A., Farmer, J.D., Farrand, W.H., Fike, D.A., Gellert, R., Ghosh, A., Glotch, T.D., Grotzinger, J.P., Hahn, B., Herkenhoff, K.E., Hurowitz, J.A., Johnson, J.R., Johnson, S.S., Jolliff, B.L., Klingelhofer, G., Knoll, A.H., Learner, Z.A., Malin, M.C., McSween Jr., H.Y., Pocock, J., Ruff, S.W., Soderblom, L.A., Squyres, S.W., Tosca, N.J., Watters, W.A., Wyatt, M.B., Yen, A., 2005. Provenance and diagenesis of the evaporite-bearing Burns formation, Meridiani Planum, Mars. Earth Planet. *Sci. Lett.* **240**, 95–121.

McSween Jr., H.Y., Treiman, A.H., 1998. Martian meteorites. In: *Planetary Materials*. In: Papike, J.J. (Ed.), *Reviews in Mineralogy*, Vol. 36. Mineralogical Society of America, Washington DC, pp. 6-1–6-53.

McSween Jr., H.Y., Arvidson, R.E., Bell III, J.F., Blaney, D.L., Cabrol, N.A., Christensen, P.R., Clark, B.C., Crisp, J., Crumpler, L.S., Des Marais, D.J., Farmer, J.D., Gellert, R., Ghosh, A., Gorevan, S., Graff, T., Grant, J., Haskin, L.A., Herkenhoff, K.E., Johnson, J.R., Jolliff, B.L., Klingelhofer, G., Knudson, A.T., McLennan, S.M., Milam, K.A., Moersch, J.E., Morris, R.V., Rieder, R., Ruff, S.W., de Souza Jr., P.A., Squyres, S.W., Wanke, H., Wang, A., Wyatt, M.B., Yen, A., Zipfel, J., 2004. Basaltic rocks analyzed by the Spirit Rover in Gusev Crater. *Science* **305**, 842–845.

Morris, R.V., Klingelhofer, G., Bernhardt, B., Schroder, C., Rodionov, D.S., de Souza Jr., P.A., Yen, A., Gellert, R., Evlanov, E.N., Foh, J., Kankeleit, E., Gutlich, P., Ming, D.W., Renz, F., Wdowiak, T., Squyres, S.W., Arvidson, R.E., 2004. Mineralogy at Gusev Crater from the Mossbauer Spectrometer on the Spirit Rover. *Science* **305**, 833–836.

Mustard, J.F., Poulet, F., Gendrin, A., Bibrin, J.-P., Langevin, Y., Gondet, B., Mangold, N., Bellucci, G., Altieri, F., 2005. Olivine and pyroxene diversity in the crust of Mars. *Science* **307**, 1594–1597.

Newsom, H.E., Hagerty, J.J., Goff, F., 1999. Mixed hydrothermal fluids and the origin of the Martian soil. *J. Geophys. Res.* **104**, 8717–8728.

Oelkers, E.H., 2001a. An experimental study of forsterite dissolution rates as a function of temperature and aqueous Mg and Si concentrations. *Chem. Geol.* **175**, 485–494.

Oelkers, E.H., 2001b. General kinetic description of multioxide silicate mineral and glass dissolution. *Geochim. Cosmochim. Acta* **65**, 3703–3719.

Parker, T.J., Gorsline, D.S., Saunders, R.S., Pieri, D.C., Scheneeberger, D.M., 1993. Coastal geomorphology of the Martian northern plains. *J. Geophys. Res.* **98**, 11061–11078.

Pokrovsky, O.S., Schott, J., 2000a. Kinetics and mechanism of forsterite dissolution at 25 °C and pH from 1 to 12. *Geochim. Cosmochim. Acta* **64**, 3313–3325.

Pokrovsky, O.S., Schott, J., 2000b. Forsterite surface composition in aqueous solutions: A combined potentiometric, electrokinetic, and spectroscopic approach. *Geochim. Cosmochim. Acta* **64**, 3299–3312.

Pollack, J.B., Kasting, J.F., Richardson, S.M., Poliakoff, K., 1987. The case for a wet, warm climate on early Mars. *Icarus* **71**, 203–224.

Presley, M.A., Christensen, P.R., 1997. Thermal conductivity measurements of particulate materials 2. Results. *J. Geophys. Res.* **102**, 6551–6566.

Rieder, R., Gellert, R., Anderson, R.C., Bruckner, J., Clark, B.C., Dreibus, G., Economou, T., Klingelhofer, G., Lugmair, G.W., Ming, D.W., Squyres, S.W., d'Uston, C., Wanke, H., Yen, A., Zipfel, J., 2004. Chemistry of rocks and soils at Meridiani Planum from the Alpha Particle X-Ray Spectrometer. *Science* **306**, 1746–1749.

Rosso, J.J., Rimstidt, J.D., 2000. A high resolution study of forsterite dissolution rates. *Geochim. Cosmochim. Acta* **64**, 797–811.

Sak, P.B., Fisher, D.M., Gardner, T.W., Murphy, K., Brantley, S.L., 2004. Rates of weathering rind formation on Costa Rican basalt. *Geochim. Cosmochim. Acta* **68**, 1453–1472.

Santelli, C.M., Welch, S.A., Westrich, H.R., Banfield, J.F., 2001. The effect of Fe-oxidizing bacteria on Fe-silicate mineral dissolution. *Chem. Geol.* **180**, 99–115.

Segura, T.L., Toon, O.B., Colaprete, A., Zahnle, K., 2002. Environmental effects of large impacts on Mars. *Science* **298**, 1977–1980.

Soderblom, L.A., Anderson, R.C., Arvidson, R.E., Bell III, J.F., Cabrol, N.A., Calvin, W.M., Christensen, P.R., Clark, B.C., Economou, T., Ehlmann, B.L., Farrand, W.H., Fike, D., Gellert, R., Glotch, T.D., Golombek, M.P., Greeley, R., Grotzinger, J.P., Herkenhoff, K.E., Jerolmack, D.J., Johnson, J.R., Jolliff, B.L., Klingelhofer, G., Knoll, A.H., Learner, Z.A., Li, R., Malin, M.C., McLennan, S.M., McSween Jr., H.Y., Ming, D.W., Morris, R.V., Rice Jr., J.W., Richter, L., Rieder, R., Rodionov, D.S., Schroder, C., Seelos IV, F.P., Soderblom, J.M., Squyres, S.W., Sullivan, R., Watters, W.A., Weitz, C.M., Wyatt, M.B., Yen, A., Zipfel, J., 2004. Soils of Eagle Crater and Meridiani Planum at the Opportunity Rover landing site. *Science* **306**, 1723–1726.

Squyres, S.W., Arvidson, R.E., Bell III, J.F., Bruckner, J., Cabrol, N.A., Calvin, W.M., Carr, M.H., Christensen, P.R., Clark, B.C., Crumpler, L.S., Des Marais, D.J., d'Uston, C., Economou, T., Farmer, J.D., Farrand, W.H., Folkner, W., Golombek, M.P., Gorevan, S., Grant, J.A., Greeley, R., Grotzinger, J.P., Haskin, L.A., Herkenhoff, K.E., Hviid, S.F., Johnson, J.R., Klingelhofer, G., Knoll, A.H., Landis, G., Lemmon, M., Li, R., Madsen, M.B., Malin, M.C., McLennan, S.M., McSween Jr., H.Y., Ming, D.W., Moersch, J.E., Morris, R.V., Parker, T.J., Rice Jr., J.W., Richter, L., Rieder, R., Sims, M., Smith, M.D., Smith, P.H., Soderblom, L.A., Sullivan, R., Wanke, H., Wdowiak, T., Wolff, M.J., Yen, A., 2004a. The Spirit Rover's Athena science investigation at Gusev Crater, Mars. *Science* **305**, 794–799.

Squyres, S.W., Grotzinger, J.P., Arvidson, R.E., Bell III, J.F., Calvin, W.M., Christensen, P.R., Clark, B.C., Crisp, J.A., Farrand, W.H., Herkenhoff, K.E., Johnson, J.R., Klingelhofer, G., Knoll, A.H., McLennan, S.M., McSween Jr., H.Y., Morris, R.V., Rice Jr., J.W., Rieder, R., Soderblom, L.A., 2004b. In situ evidence for an ancient aqueous environment at Meridiani Planum, Mars. *Science* **306**, 1709–1714.

Stopar, J.D., Lawrence, S.J., Lentz, R.C.F., Taylor, G.J., 2005. Preliminary analysis of nakhlite MIL 03346, with a focus on secondary alteration. Lunar and Planetary Science Conference XXXVI, Abstract #1547.

Tosca, N.J., Hurowitz, J.A., Meltzer, L., McLennan, S.M., Schoonen, M.A.A., 2004. Olivine weathering on Mars: Getting back to basics. Lunar and Planetary Science Conference XXXV, Abstract #1043.

Treiman, A.H., 2005. The nakhlite meteorites: Augite-rich igneous rocks from Mars. *Chemie der Erde* **65**, 203–270.

Velbel, M.A., 1993. Constancy of silicate-mineral weathering-rate ratios between natural and experimental weathering: Implications for hydrologic control of difference in absolute rates. *Chem. Geol.* **105**, 89–99.

Welch, S.A., Banfield, J.F., 2002. Modification of olivine surface morphology and reactivity by microbial activity during chemical weathering. *Geochim. Cosmochim. Acta* **66**, 213–221.

White, A.F., Brantley, S.L., 2003. The effect of time on the weathering of silicate minerals: Why do weathering rates differ in the laboratory and field? *Chem. Geol.* **202**, 479–506.

Wogelius, R.A., Walther, J.V., 1991. Olivine dissolution at 25 °C: Effects of pH, CO_2, and organic acids. *Geochim. Cosmochim. Acta* **55**, 943–954.

Wogelius, R.A., Walther, J.V., 1992. Olivine dissolution kinetics at near-surface conditions. *Chem. Geol.* **97**, 101–112.

Yen, A.S., Gellert, R., Schroder, C., Morris, R.V., Bell III, J.F., Knudson, A.T., Clark, B.C., Ming, D.W., Crisp, J.A., Arvidson, R.E., Blaney,

D.L., Bruckner, J., Christensen, P.R., Des Marais, D.J., de Souza Jr., P.A., Economou, T.E., Ghosh, A., Hahn, B.C., Herkenhoff, K.E., Haskin, L.A., Hurowitz, J.A., Jolliff, B.L., Johnson, J.R., Klingelhofer, G., Madsen, M.B., McLennan, S.M., McSween Jr., H.Y., Lutz, R., Rieder, R., Rodionov, D., Soderblom, L., Squyres, S.W., Tosca, N.J., Wang, A., Wyatt, M.B., Zipfel, J., . An integrated view of the chemistry and mineralogy of Martian soils. *Nature* **436**, 49–54.